ORIGINAL ARTICLE

Rose Bengal sensitized bilayered photoanode of nano-crystalline TiO$_2$–CeO$_2$ for dye-sensitized solar cell application

Suhail A. A. R. Sayyed[1,2] · Niyamat I. Beedri[1] · Vishal S. Kadam[1] ·
Habib M. Pathan[1]

Abstract The present work deals with the study of TiO$_2$–CeO$_2$ bilayered photoanode with low-cost Rose Bengal (RB) dye as sensitizer for dye-sensitized solar cell application. The recombination reactions are reduced in bilayered TiO$_2$–CeO$_2$ photoanode as compared to the single-layered CeO$_2$ photoanode. Once the electrons get transferred from lowest unoccupied molecular orbital level of RB dye to the conduction band (CB) of TiO$_2$, then the possibilities of recombination of electrons with oxidized dye molecules or oxidized redox couple are reduced. This is because the CB position of CeO$_2$ is higher than that of TiO$_2$, which blocks the path of electrons. The electrochemical impedance spectroscopy (EIS) analysis shows negative shift in frequency for bilayered TiO$_2$–CeO$_2$ photoanode as compared to CeO$_2$ photoanode. Hence, in bilayered photoanode lifetime of electrons is more than in single-layered photoanode, confirming reduction in recombination reactions. The X-ray diffraction patterns confirm both anatase TiO$_2$ and CeO$_2$ with crystalline size using Scherrer formula as 24 and 10 nm, respectively. The scanning electron microscopy images of photoanode show the porous structure useful for dye adsorption. The presence of Ti and Ce is confirmed by electron diffraction studies. The band gap values for TiO$_2$ and CeO$_2$ were calculated as 3.20 and 3.11 eV, respectively, using diffused reflectance spectroscopy. The bilayered TiO$_2$–CeO$_2$ photoanode showed open-circuit voltage (V_{OC}) $\sim$500 mV and short-circuit photocurrent density (J_{SC}) $\sim$0.29 mA/cm^2 with fill factor (FF) $\sim$62.17 %. There is increase in V_{OC} and J_{SC} values by 66.67 and 38.10 %, respectively, compared to RB-sensitized CeO$_2$ photoanode.

Keywords Dye-sensitized solar cell · Photoanode · Rose Bengal dye · TiO$_2$–CeO$_2$

✉ Habib M. Pathan
pathan@physics.unipune.ac.in

Suhail A. A. R. Sayyed
sasayyed81@gmail.com

[1] Advanced Physics Laboratory, Department of Physics, Savitribai Phule Pune University, Pune 411 007, India

[2] Department of Physics, B.P.H.E. Society's Ahmednagar College, Ahmednagar 414 001, India

Introduction

Solar energy can solve the problem of energy crisis. Although silicon-based and thin-film solar cells are having good efficiencies, they are costly, which make them away from common people's reach. Moreover, toxic materials such as cadmium used in thin-film solar cells are harmful. DSSCs are low cost, environment friendly and hence, consumer adaptable solution.

TiO$_2$ has been widely used as a photoanode material in DSSCs, since its discovery by O'Regan and Gratzel (1991) as compared to other wide band gap semiconducting metal oxides such as SnO$_2$ (Bedja et al. 1994; Ferrere et al. 1997), ZnO (Redmond et al. 1994; Rensmo et al. 1997; Rao and Bahadur 1997; Keis et al. 1999), Nb$_2$O$_5$ (Sayama et al. 1998; Guo and Aegerter 1999), CeO$_2$ (Turkovic and Crnjak 1997) and SrTiO$_3$ (El Zayat et al. 1998). The DSSCs are based on the sensitization of wide band gap material to visible and near-infrared light by adsorbed dye molecules to the photoanode. Efforts of researchers are focused on the solar conversion efficiency improvement. Some

undesirable reactions like recombination of injected electrons either with the oxidized sensitizer or with the oxidized redox couple at TiO_2 surface (Nazeeruddin et al. 2011) result in loss in the cell efficiency.

In order to reduce recombination rate, different research groups are using different nano-composites or bilayered photoanode. Tripathi and Chawla (2014) used a CeO_2–TiO_2 nano-composite photoanode sensitized with betacyanin natural dye in order to reduce recombination rate by providing inherent energy barrier. Upadhayay et al. (2014) have used natural dye-sensitized CeO_2–TiO_2 admixed photoanode to reduce the charge recombination rate by providing energy barrier at the interface between the photoanode and electrolyte. According to Mangesh et al. (2009), mixing oxides of rare earth elements, specially CeO_2 with TiO_2, reduces the recombination rate at the TiO_2 interface. For this they have used photocatalytic behavior of CeO_2–TiO_2 system for the degradation of methylene blue. Greene et al. (2007) tried ZnO–TiO_2 core shell nano-rod combination for solar cells. Maheshwari and Venkatchalam (2014) studied enhanced efficiency and improved photocatalytic activity of 1:1 composite mixture of TiO_2 nanoparticles and nanotubes in DSSCs. Kang et al. (2002) studied the improvement of the photocurrent and conversion efficiency of DSSCs by homogeneously incorporating large titanium silicate particles ($\sim$500 nm long) in the TiO_2 film electrodes. Yu et al. (2012) developed a new type of bilayered photoanode with TiO_2 and cubic CeO_2 nanoparticles as mirror-like scattering thin layers via screen printing technique for DSSCs. Rai et al. (2014) have used CeO_2 quantum-dot-functionalized ZnO nano-rod photoanode for DSSC application.

In the present study, our aim is to improve the efficiency of CeO_2-based DSSCs. For this, we have used low-cost RB sensitized bilayered TiO_2–CeO_2 photoanode. The LUMO level of RB dye is at -3.7 eV (Oku et al. 2011), CB of CeO_2 is at -0.53 eV (Elaziouti et al. 2014) and CB of TiO_2 is at -0.29 eV (Gratzel 2001). Thus, the electron transfer from LUMO level of RB dye to CB of TiO_2 is facilitated through CB of CeO_2. Also, the electron transfer directly from LUMO level of RB dye to the CB of TiO_2 is possible. Moreover, CeO_2 acts as a blocking layer to reduce the electron recombination. Although the efficiency is less for low-cost dyes, cost per watt will be reduced, if we achieve moderate efficiency.

Experimental procedure

Bilayered TiO_2–CeO_2 photoanode fabrication

Nano-titanium dioxide (TiO_2) powder was purchased from Nvis Technology. Cerium nitrate ($Ce(NO_3)_3 \cdot 6H_2O$) and RB dye were purchased from HPLC, and ammonium hydroxide solution (20 %, NH_4OH) was purchased from Thomas baker.

To make TiO_2 paste, 0.5 g of TiO_2 powder was mixed with 0.4 g ethyl cellulose, 2.5 g anhydrous terpineol and 5 ml ethyl alcohol. The mixture was properly mixed with mortar and pestle to form a uniform paste. Then, this paste was deposited on fluorine-doped tin oxide (FTO) glass using doctor blade method. After 20–30 min of drying, samples were annealed for 1 h at 250 °C.

The nano-crystalline CeO_2 powder was prepared using $Ce(NO_3)_3 \cdot 6H_2O$ and NH_4OH, where $Ce(NO_3)_3 \cdot 6H_2O$ was used as a source of Ce^{4+} and NH_4OH was the precipitant. The precipitated powder obtained after evaporation of water was annealed at 450 °C to obtain nano-crystalline CeO_2 powder.

By using above-synthesized CeO_2 powder, CeO_2 paste was prepared by the similar procedure as that of TiO_2 paste was prepared. And the CeO_2 film was deposited on the annealed TiO_2 layer, using doctor blade method. After 20–30 min of drying, samples were kept for annealing for 1 h at 450 °C. These samples were characterized by SEM (Model No. JEOL–JSM6360-A). TiO_2 and CeO_2 films were separately characterized by using XRD pattern (Model No. D-8 Advance Bruker AXS, Germany) equipped with a monochromator Cu-Kα radiation source ($\lambda = 1.54$ Å) and DRS by using UV–Vis absorption spectrophotometer (Jasco Model: V-670).

Fabrication of solar cell

All annealed films were kept immersed in 0.3 mM RB dye in ethanol for 24 h to adsorb dye on the surface of photoanode. To prepare the counter electrode, the FTO was washed with acetone, water and ethanol. After removing contaminants, carbon-coated counter electrode was prepared on the conductive side of the FTO substrate by using mild flame of candle.

To fabricate the solar cell, few drops of electrolyte solution (iodide/tri-iodide redox mediator) were added to dye-loaded TiO_2–CeO_2 photoanode before covering it with counter electrode (carbon-coated FTO). Then, both the photoanode and the counter electrodes were clamped together using binder clips. Performance of the cells was studied by using the photocurrent density–voltage (JV) characteristics. The cells were tested for voltage against time for different loads. EIS analysis (Bode plot) was performed for RB-sensitized single-layered TiO_2, CeO_2 photoanode and bilayered TiO_2–CeO_2 photoanode. To test the stability of such DSSCs, the V_{OC} and J_{SC} values were measured for 10 days.

Results and discussion

XRD analysis of TiO₂ and CeO₂

The presence nano-crystalline anatase TiO_2 was confirmed by XRD pattern (Fig. 1a). As per Joint Committee on Powder Diffraction Standards (JCPDS 21-1272), there are ten peaks at $2\theta = 25.3°, 36.9°, 37.8°, 38.5°, 48.0°, 53.9°, 55.0°, 62.0°, 62.7°$ and $78.2°$ with corresponding miller planes at (101), (110), (004), (200), (105), (211), (204), (116), (220) and (215). The presence of nano-crystalline CeO_2 was confirmed by XRD pattern (Fig. 1b). As per JCPDS No. 81-0792, there are eight peaks observed at $2\theta = 28.6°, 33.1°, 47.5°, 56.4°, 59.1°, 68.1°, 76.8°$ and $79.1°$ which are assigned to diffraction from the (111), (200), (220), (311), (222), (400), (331) and (420) planes, respectively, for cubic structure of CeO_2.

The average crystalline size (D) of the TiO_2 and CeO_2 was estimated by using Scherrer formula (Azaroff 1968).

$$D = \frac{0.89\lambda}{\beta \cos \theta} \tag{1}$$

where λ is wavelength of X-rays ($\lambda = 1.54$ Å), β is full width in radians at half maximum of diffraction peaks, and θ is the Bragg's angle of the X-ray pattern at maximum intensity. The crystalline size of TiO_2 and CeO_2 was found as ~ 24 and ~ 10 nm, respectively.

Optical properties of TiO₂ and CeO₂ films

The DRS absorption data obtained from UV–Vis spectrophotometer is used to calculate the band gap. As shown in Fig. 2, the band gap of TiO_2 (annealed at 250 °C) and CeO_2 (annealed at 450 °C) films was found to be 3.20 and 3.11 eV, respectively. Figure 2 shows the absorption peaks nearly at 320 and 350 nm for TiO_2 and CeO_2, respectively.
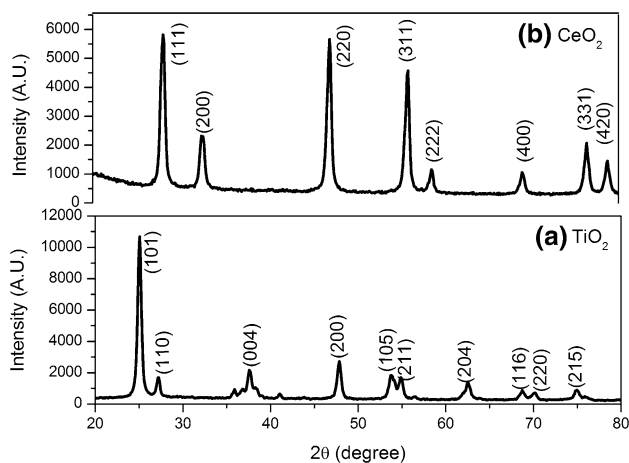

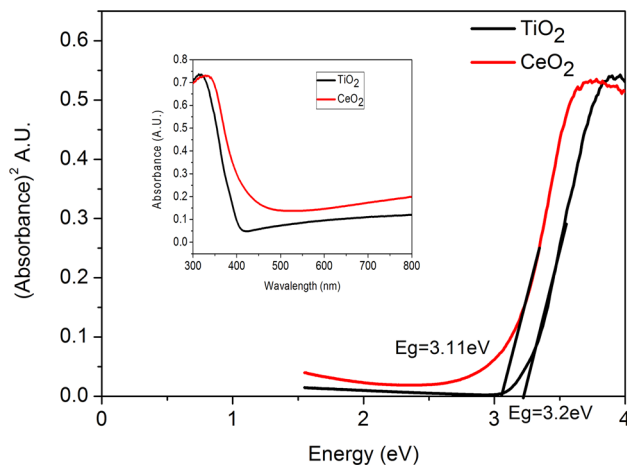**Fig. 1** XRD pattern of **a** TiO_2 **b** CeO_2 samples

Fig. 2 Optical absorption spectra and band gap of TiO_2 and CeO_2 films
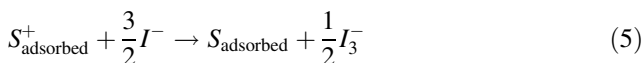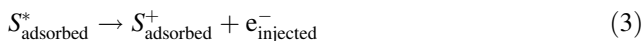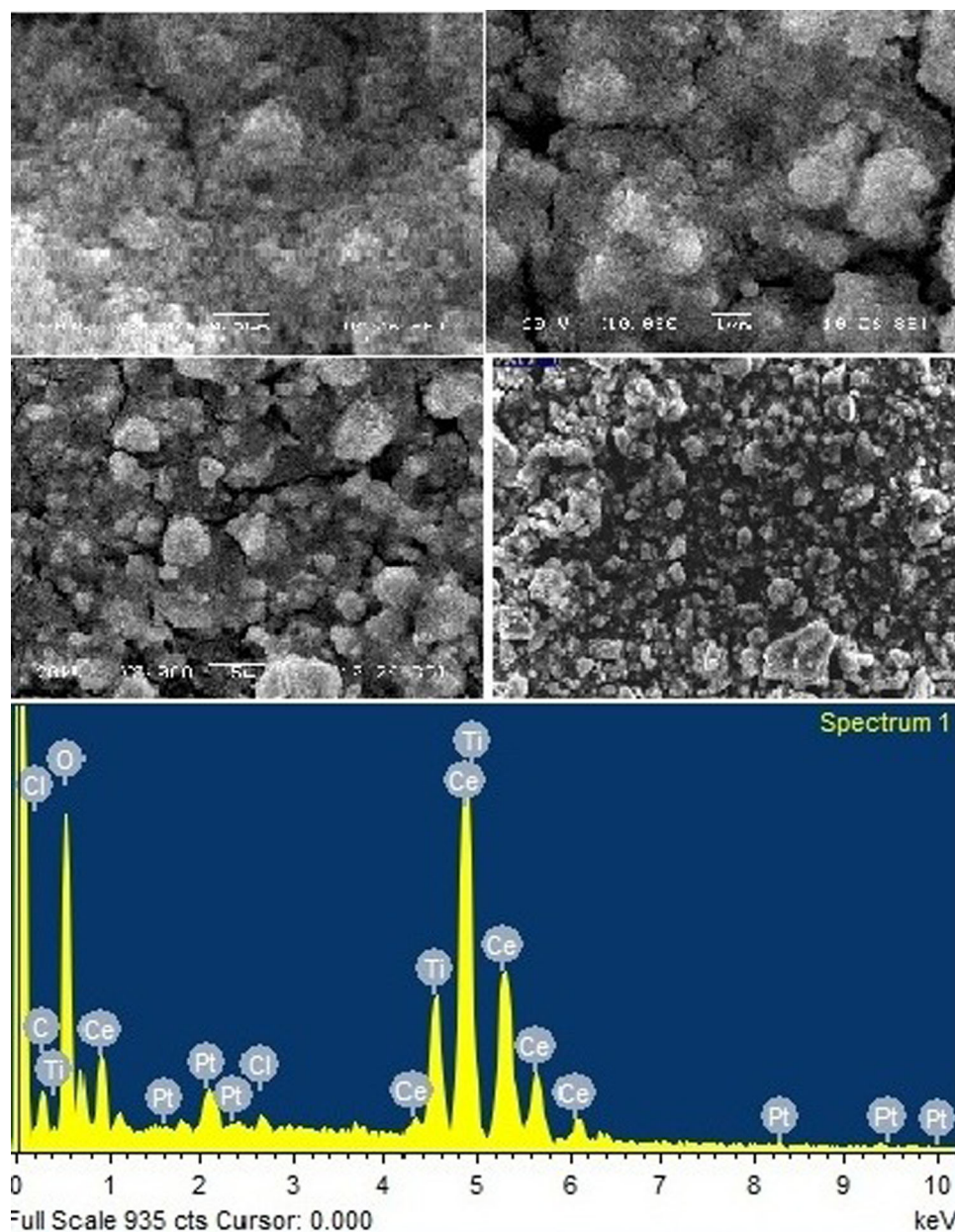
SEM and EDS of TiO₂–CeO₂ photoanode

According to Gratzel (2003), the heart of the DSSC system is a mesoporous oxide layer composed of nanometer-sized particles which have been sintered together to allow for electronic conduction to take place. The surface morphology plays the most important role in dye adsorption in DSSCs. The SEM micrographs, as shown in Fig. 3, are obtained to study the surface morphology of TiO_2–CeO_2 photoanode. The sample possesses network of aggregated sphere like morphology with pores of size roughly in the range 60–80 nm. The morphology of photoanode is porous and rough, useful for maximum dye adsorption. EDS confirms the presence of Ti and Ce (Fig. 3), which supports the XRD results.

JV characteristics of DSSC

A charge transfer process in DSSC based on RB-sensitized TiO_2–CeO_2 photoanode can be explained in similar way as explained by Rai et al. (2014). The charge transfer process is shown in Fig. 4. Initially, by absorbing the photons the RB dye gets sensitized. And electrons from highest occupied molecular orbital (HOMO) get transferred to excited state, i.e., LUMO. The CB position of CeO_2 (-0.53 eV) (Elaziouti et al. 2014) lies below LUMO level of RB dye (-3.7 eV) (Oku et al. 2011). Hence, the electrons in LUMO level are injected quickly into the CB of CeO_2, get transferred to the CB of TiO_2 (-0.29 eV) (Gratzel 2001) and finally transferred to FTO substrate where they are utilized for the conduction. Since CB of CeO_2 is higher than that of TiO_2, the layer of CeO_2 acts as blocking layer for electrons to recombine either with dye or with electrolyte. The corresponding mechanism of transportation of electrons is represented according to Nazeeruddin et al. (2011) by Eqs. (2)–(5).

Fig. 3 SEM images and EDS of bilayered TiO_2–CeO_2 photoanode

$$S_{adsorbed} + hv \rightarrow S^*_{adsorbed} \qquad (2)$$

$$S^*_{adsorbed} \rightarrow S^+_{adsorbed} + e^-_{injected} \qquad (3)$$

$$I_3^- + 2e^-_{cathode} \rightarrow 3I^-_{cathode} \qquad (4)$$

$$S^+_{adsorbed} + \frac{3}{2}I^- \rightarrow S_{adsorbed} + \frac{1}{2}I_3^- \qquad (5)$$

$$S^+_{adsorbed} + e^-_{TiO_2} \rightarrow S_{adsorbed} \qquad (6)$$

$$I_3^- + 2e^-_{TiO_2} \rightarrow 3I^-_{anode} \qquad (7)$$

where $S_{adsorbed}$, $S^*_{adsorbed}$ and $S^+_{adsorbed}$ correspond to ground state, excited and oxidized molecules of RB dye, respectively.

The injected electrons diffuse through CeO_2–TiO_2 porous network and transfer through external load toward counter electrode. The oxidized dye is quickly reduced back to its original state by reduced redox species I^- in the electrolyte which in turn become the oxidized redox species I_3^-.

Some undesirable reactions may take place in case of single-layered wide band gap material resulting in losses in the cell efficiency. They are the recombination of the injected electrons (Fig. 4 dotted lines) either with oxidized sensitizer (Eq. 6) or with the oxidized redox couple at the monolayer wide band gap material surface (Eq. 7). The recombination reactions (Eqs. 6 and 7) are reduced in bilayered TiO_2–CeO_2 photoanode.
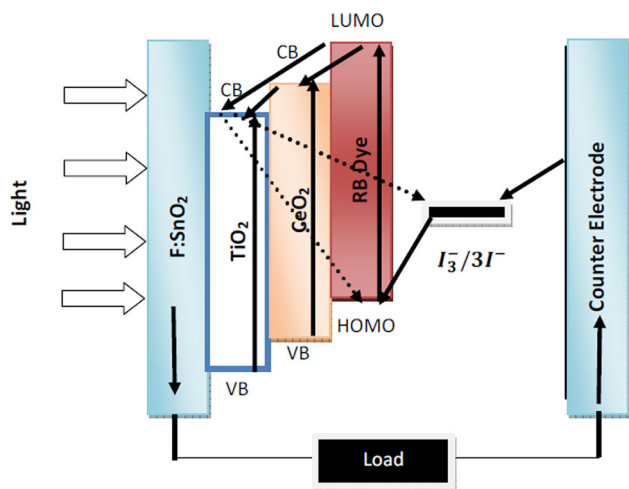
Fig. 4 Schematic of processes involved in RB-sensitized bilayered TiO$_2$–CeO$_2$ -based DSSC
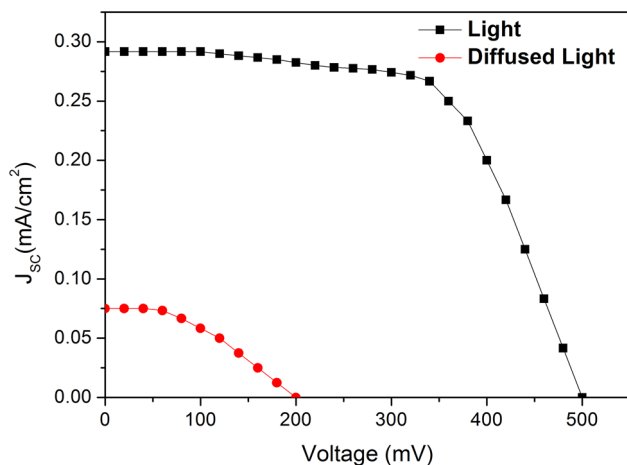

Fig. 5 Photocurrent density–voltage (J–V) characteristics of DSSCs based on RB sensitized bilayered TiO$_2$–CeO$_2$ photoanode

Table 1 Solar cell parameters for RB-sensitized bilayered TiO$_2$–CeO$_2$ photoanode

Parameter	Light (30 mW/cm^2)	Diffused light (0.3 mW/cm^2)
V_{oc} (mV)	500	200
I_{SC} (mA)	0.04	0.009
V_{max} (mV)	320	100
I_{max} (mA)	0.03	0.007
J_{SC} (mA/cm^2)	0.29	0.08
Cell area (cm^2)	0.12	0.12
Fill factor	62.17 %	40.00 %

Table 2 Comparison of solar cell parameter of RB-sensitized TiO$_2$–CeO$_2$ photoanode with RB-sensitized CeO$_2$ photoanode under light (30 mW/cm^2)

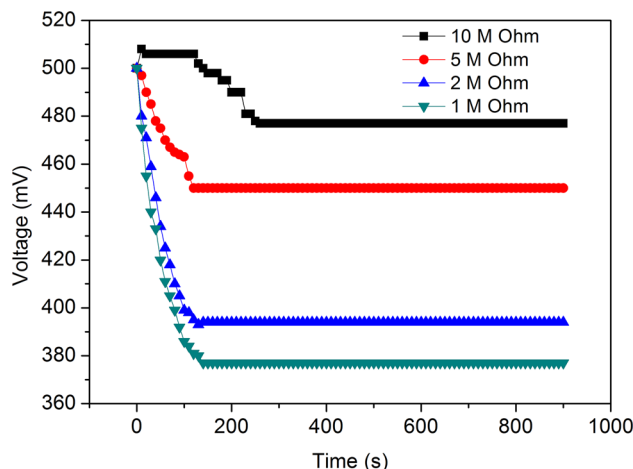| Parameter	CeO$_2$	TiO$_2$–CeO$_2$	% Increase
V_{OC} (mV)	300	500	66.67
J_{SC} (mA/cm^2)	0.21	0.29	38.10
Fill factor	58.67 %	62.17 %	03.50

Fig. 6 Voltage–time graph at different loads of DSSCs based on RB-sensitized bilayered TiO$_2$-CeO$_2$ photoanode
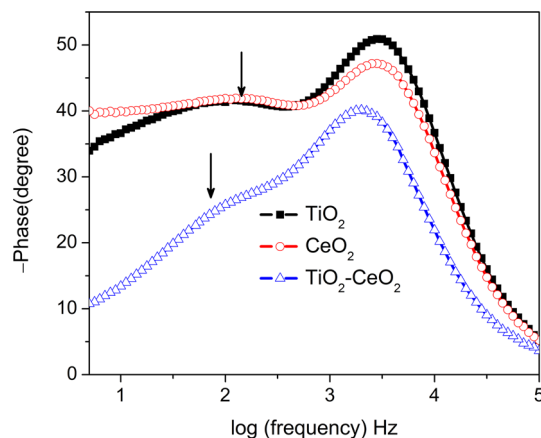

Fig. 7 Bode plot for RB-sensitized single-layered TiO$_2$, CeO$_2$ and bilayered TiO$_2$–CeO$_2$ photoanode

cell performance was observed for the optimized dye adsorption time (DAT) of 24 h. The best-performing cell shows V_{OC} ~500 mV and J_{SC} ~0.29 mA/cm^2 with fill factor of 62.12 %. Table 1 summarizes the performance of cell under light (30 mW/cm^2) and diffused light (0.3 mW/cm^2) conditions. As given in Table 2, there is 66.67 and 38.10 % increase in V_{OC} and J_{SC} values, respectively, compared to RB-sensitized CeO$_2$ photoanode. We are getting better results as compared to Turkovic and Crnjak

Figure 5 shows the J–V characteristics of DSSCs based on TiO$_2$–CeO$_2$ photoanode. The performance of cell is improved as the recombination reactions are reduced. The

([1997](#)), in which they have discussed ruthenium dye-sensitized CeO_2 showing $V_{OC} \sim 60$ mV and $J_{SC} \sim 25$ nA/cm^2. Comparing with other groups (Tripathi and Chawla [2014](#); Upadhyay et al. [2014](#); Yu et al. [2012](#)) work on bilayered TiO_2–CeO_2 or mixed nano-composite photoanode, we are getting less values of V_{OC} and J_{SC}. As we are using low-cost, easily available and environment-friendly RB dye, the cost per unit watt will reduce.

Figure [6](#) shows the voltage against time graphs for different loads, which indicate that the cells are having good performance. Figure [7](#) shows the EIS analysis (Bode plot) for RB-sensitized single-layered TiO_2, CeO_2 and bilayered TiO_2–CeO_2 photoanode. For bilayered photoanode, there is negative shift in frequency as compared to single-layered photoanode. Thus, there is increase in lifetime of electrons in bilayered photoanode, confirming reduction in recombination reactions. As a result, there is improvement in the performance of the cell. The cells were tested for stability for 10 days, which showed stable performance.

Conclusion

In conclusion, the RB sensitized bilayered nano-crystalline TiO_2–CeO_2 photoanode was successfully fabricated and tested. The best performance of cell for 24 h DAT shows $V_{OC} \sim 500$ mV and $J_{SC} \sim 0.29$ mA/cm^2 with FF ~ 62.12 %. There is 66.67 and 38.10 % increase in V_{OC} and J_{SC} values, respectively, compared to CeO_2 photoanode. The performance of cell can be further improved by controlling different parameters. The cells show good performance for different loads and are tested for 10 days having the stable performance.

References

Azaroff LV (1968) Elements of X-ray crystallography. McGraw-Hill, New York, p 552

Bedja I, Hotchandani S, Kamat PV (1994) Preparation and photoelectrochemical characterization of thin SnO_2 nanocrystalline semiconductor films and their sensitization with bis(2,2′-bipyridine)(2,2′-bipyridine-4,4′-dicarboxylic acid)ruthenium(II) complex. J Phys Chem 98:4133–4140

El Zayat MY, Saed AO, El-Dessouki MS (1998) Photoelectrochemical properties of dye sensitized Zr-doped $SrTiO_3$ electrodes. Int J Hydrogen Energy 23:259–266

Elaziouti A, Laouedj N, Bekka A, Vannier RN (2014) Preparation and characterization of P–N heterojunction $CuBi_2O_4$/CeO_2 and its photocatalytic activities under UVA light irradiation. Sci Technol A 39:9–22

Ferrere S, Zaban A, Gregg B (1997) Dye sensitization of nanocrystalline tin oxide by perylene derivatives. J Phys Chem B 101:4490–4493

Gratzel M (2001) Photoelectrochemical cells. Nature 414(15):338–344

Gratzel M (2003) Dye-sensitized solar cells. J Photochem Photobiol C 4:145–153

Greene LE, Law M, Yuhas BD, Yang P (2007) ZnO–TiO_2 core–shell nanorod/P3HT solar cells. Phys Chem C Lett 111:18451–18456

Guo P, Aegerter MA (1999) RU(II) sensitized Nb_2O_5 solar cell made by the sol–gel process. Thin Solid Films 351:290–294

Kang MG, Park NG, Chang SH, Choi SH, Kim KJ (2002) Enhanced photocurrent of Ru(II)-dye sensitized solar cells by incorporation of titanium silicalite-2 in TiO_2 film. Bull Korean Chem Soc 23(1):140–142

Keis K, Vayssieres L, Lindquist SE, Hagfelt A (1999) Nanostructured ZnO electrodes for photovoltaic applications. Nanostruct Mater 12:487–490

Maheshwari D, Venkatchalam P (2014) Enhanced efficiency and improved photocatalytic activity of 1:1 composite mixture of TiO_2 nanoparticles and nanotubes in dye-sensitized solar cell. Bull Mater Sci 37(6):1489–1496

Mangesh G, Vishwanathan B, Vishwanath RP, Varadarajan TK (2009) Photocatalytic behavior of CeO_2–TiO_2 system for the degradation of methylene blue. Indian J Chem 48A:480–488

Nazeeruddin MK, Baranoff E, Gratzel M (2011) Dye-sensitized solar cells: a brief overview. Sol Energy 85:1172–1178

O'Regan B, Grätzel M (1991) A low-cost, high-efficiency solar cell based on dye-sensitized colloidal TiO_2 films. Nature 353:737–740

Oku T, Kakuta N, Kobayashi K, Suzuki A, Kikuchi K (2011) Fabrication and characterization of TiO2 based dye sensitized solar cells. Prog Nat Sci Mater Int 21:122–126

Rai P, Khan R, Ko KJ, Lee JH, Yu YT (2014) CeO_2 quantum dot functionalized ZnO nanorods photoanode for DSSC applications. J Mater Sci Mater Electron 25(7):2872–2877

Rao TN, Bahadur LJ (1997) Photoelectrochemical studies on dye-sensitized particulate ZnO thin-film photoelectrodes in nonaqueous media. J Electrochem Soc 144:179–185

Redmond G, Fitzmaurice D, Grätzel M (1994) Visible light sensitization by cis-bis(thiocyanato)bis(2,2′-bipyridyl-4,4′-dicarboxylato)ruthenium(II) of a transparent nanocrystalline ZnO film prepared by sol–gel techniques. Chem Mater 6:686–691

Rensmo H, Keis K, Lindström H, Sodergren S, Solbrand A, Hagfelt A, Lindquist SE, Wang LN, Muhammed MJ (1997) High light-to-energy conversion efficiencies for solar cells based on nanostructured ZnO electrodes. Phys Chem B 101:2598–2601

Sayama K, Sugihara H, Arakawa H (1998) Photoelectrochemical properties of a porous Nb_2O_5 electrode sensitized by a ruthenium dye. Chem Mater 10:3825–3832

Tripathi M, Chawla P (2014) CeO_2–TiO_2 photoanode for solid state natural dye-sensitized solar cell. Ionics 21:541–546

Turkovic A, Crnjak Z (1997) Dye-sensitized solar cell with CeO$_2$ and mixed CeO$_2$/SnO$_2$ photoanodes. Sol Energy Mater Sol Cells 45:275–281

Upadhyay R, Tripathi M, Chawla P, Pandey A (2014) Performance of CeO$_2$–TiO$_2$-admixed photoelectrode for natural dye-sensitized solar cell. J Solid State Electrochem 18(7):1889–1892

Yu H, Bai Y, Zong X, Tang F, Max LuGQ, Wang L (2012) Cubic CeO$_2$ nanoparticles as mirror-like scattering layers for efficient light harvesting in dye-sensitized solar cells. Chem Commun 48:7386–7388